Rate Constants for Reactions of
Hydrazine Fuels with O(^{3}P)

Prepared by

V. I. LANG
Space and Environment Technology Center
Technology Operations

DTIC
S ELECTE
JUL 15 1992
D
A

15 February 1992

Prepared for

SPACE SYSTEMS DIVISION
AIR FORCE SYSTEMS COMMAND
Los Angeles Air Force Base
P. O. Box 92960
Los Angeles, CA 90009-2960

Engineering and Technology Group

THE AEROSPACE CORPORATION
El Segundo, California

92

92-18653

MARTIN K. WILLIAMS, Capt, USAF
MOIE Program Manager

MICHAEL J. GOODMAN
Major, USAF

REPORT DOCUMENTATION PAGE

1a. REPORT SECURITY CLASSIFICATION Unclassified		1b. RESTRICTIVE MARKINGS	
2a. SECURITY CLASSIFICATION AUTHORITY		3. DISTRIBUTION/AVAILABILITY OF REPORT Approved for public release; distribution unlimited	
2b. DECLASSIFICATION/DOWNGRADING SCHEDULE			
4. PERFORMING ORGANIZATION REPORT NUMBER(S) TR-0091(6940-07)-2		5. MONITORING ORGANIZATION REPORT NUMBER(S) SSD-TR-92-20	
6a. NAME OF PERFORMING ORGANIZATION The Aerospace Corporation Technology Operations	6b. OFFICE SYMBOL (If applicable)	7a. NAME OF MONITORING ORGANIZATION Space Systems Division	
6c. ADDRESS (City, State, and ZIP Code) El Segundo, CA 90245-4691		7b. ADDRESS (City, State, and ZIP Code) Los Angeles Air Force Base Los Angeles, CA 90009-2960	
8a. NAME OF FUNDING/SPONSORING ORGANIZATION	8b. OFFICE SYMBOL (If applicable)	9. PROCUREMENT INSTRUMENT IDENTIFICATION NUMBER F04701-88-C-0089	
8c. ADDRESS (City, State, and ZIP Code)		10. SOURCE OF FUNDING NUMBERS	

	PROGRAM ELEMENT NO.	PROJECT NO.	TASK NO.	WORK UNIT ACCESSION NO.

11. TITLE (Include Security Classification)

Rate Constants for Reactions of Hydrazine Fuels with O(^{3}P)

12. PERSONAL AUTHOR(S)
Lang, Valerie I.

13a. TYPE OF REPORT	13b. TIME COVERED FROM _____ TO _____	14. DATE OF REPORT (Year, Month, Day) 1992 February 15	15. PAGE COUNT 22

16. SUPPLEMENTARY NOTATION

17. COSATI CODES

FIELD	GROUP	SUB-GROUP

18. SUBJECT TERMS (Continue on reverse if necessary and identify by block number)

Hydrazine, Rate constant

19. ABSTRACT (Continue on reverse if necessary and identify by block number)

Room temperature rate constants for the reactions of three hydrazine fuels with O(^{3}P) were measured. A laser-photolysis resonance fluorescence technique was used in the experiments. The reactions were monitored by the decay of 131 nm, O(^{3}S-^{3}P) resonance fluorescence under both high pressure (~50 Torr) and low pressure (1 to 3 Torr) conditions. The measured rate constants were 0.99 ($\pm$0.12) x 10^{-11} cm^3 molecule^{-1} s^{-1} for N$_2$H$_4$, 1.6 ($\pm$0.34) x 10^{-11} cm^3 molecule^{-1} s^{-1} for CH$_3$HN$_2$H$_2$, and 2.3 ($\pm$0.34) x 10^{-11} cm^3 molecule^{-1} s^{-1} for (CH$_3$)$_2$N$_2$H$_2$, all at 296K. The rate constants increase with the number of hydrogen atoms per hydrazine molecule.

20. DISTRIBUTION/AVAILABILITY OF ABSTRACT [X] UNCLASSIFIED/UNLIMITED ☐ SAME AS RPT. ☐ DTIC USERS	21. ABSTRACT SECURITY CLASSIFICATION Unclassified	
22a. NAME OF RESPONSIBLE INDIVIDUAL	22b. TELEPHONE (Include Area Code)	22c. OFFICE SYMBOL

DD FORM 1473, 84 MAR   83 APR edition may be used until exhausted.
All other editions are obsolete.

PREFACE

The author would like to thank T. Hayhurst for preliminary experimental work in the subject area, M. Osibov for his contributions in the laboratory, P. F. Zittel for data acquisition software, and T. Van Zandt for designing the preamplifier.

1

CONTENTS

FIGURES

TABLES

INTRODUCTION

Unburned liquid rocket propellants are often ejected into the atmosphere at altitudes where ground-state atomic oxygen is a predominant species. In addition to anhydrous hydrazine (N_2H_4), two substituted derivatives, monomethylhydrazine ($CH_3HN_2H_2$) and unsymmetrical dimethylhydrazine (($CH_3)_2N_2H_2$) are commonly used as propellants. Chemiluminescent emission from the reaction of N_2H_4 with oxygen atoms was first observed in 1956.[1,2] The emitting species were identified as excited NH, NH_2, OH, and NO. In the early work, it was also noted that the reaction between N_2H_4 and atomic oxygen was very fast.[1,2,3] A complete understanding of the mechanisms and kinetics of the primary atmospheric reactions of each of the hydrazine species is needed to fully describe their distinct chemiluminescent signatures.

The reaction chemistry of N_2H_4 has been studied in more detail than that of the other hydrazine-type fuels. Two kinetic studies of the N_2H_4 and O atom reaction have been performed by Gehring et al..[4,5] They reported the rate coefficient of the reaction,

$$O + N_2H_4 \rightarrow N_2H_2 + H_2O \qquad (1)$$

in the Arrhenius form as

$$k_1 = 8.5 \times 10^{13} \exp\left(-\frac{1200 \; cal/mole}{RT}\right) cm^3 mol^{-1} s^{-1} \qquad (2)$$

and later modified the pre-exponential coefficient to 6.3×10^{13}. The latter value corresponds to a rate constant at 296 K of 1.4×10^{-11} cm^3 molecule^{-1} s^{-1}. The experiments were done in a fast-flow reactor with electron spin resonance and mass spectrometry detection. Shane and Brennen[6] estimated the reaction rate constant to be considerably slower, $3.0 (\pm 1.5) \times 10^{-12}$ cm^3 molecule^{-1} s^{-1} at 295 K.

There have been no rate constants previously reported for the reactions of the methylated hydrazines with atomic oxygen. The primary reaction step may be hydrogen abstraction, similar to Reaction (1),[4,7] or attack at the methyl groups.[8]

The purpose of this work was to compare the room temperature reactivity of N_2H_4, $CH_3HN_2H_2$, and ($CH_3)_2N_2H_2$ towards O(^{3}P). The rate constants for each of the three primary reactions are reported, and in the case of N_2H_4 our result is compared to the previous results of Gehring et al.[4,5] and to that of Shane and Brennen[6]. Our experimental technique of laser photolysis-resonance fluorescence was specific to monitoring ground-state atomic oxygen.

5

EXPERIMENTAL

One of the greatest difficulties associated with performing kinetic studies on hydrazine-type compounds is their rapid decomposition on the surfaces of many common laboratory materials. However, lists of hydrazine-compatible substances have been published.[9,10] With these guidelines, our experimental apparatus was designed to prevent loss of hydrazine in any part of the system prior to reaction with the O atoms. In addition, kinetic experiments in which only the hydrazine concentration is monitored are prone to result in reaction rates that are too fast if any portion of the hydrazine reacts on the walls or with contaminants such as water vapor. This bias was eliminated in our experiments by observing the decay of the other reactant, $O(^3P)$. Using our technique, any loss of hydrazine reactant would result in an apparent O atom decay rate that is slower than the actual reaction rate with hydrazine. Under the current experimental conditions there were no loss processes for the $O(^3P)$ atoms that were kinetically comparable to the reaction with hydrazine.

Anhydrous N_2H_4, $CH_3HN_2H_2$, and $(CH_3)_2N_2H_2$ liquids were obtained from Aldrich with stated purities of 98%, 99%, and 98%, respectively, and from SIGMA (N_2H_4) with a stated purity of 98.8%. Commercial N_2 (Air Products UHP, 99.999%) and O_2 (MG Industries, 99.999%) were used without further purification. One percent hydrazine vapor (N_2H_4, $CH_3HN_2H_2$ or $(CH_3)_2N_2H_2$) mixtures in N_2 diluent gas were prepared in a 30-liter pyrex manifold. The liquid hydrazine was handled under a N_2 purge before it entered the manifold, and then purified by several freeze/thaw cycles at dry ice/acetone temperatures. The hydrazine vapor pressure and the carrier gas pressure were measured using a 1000-Torr pressure manometer (Edwards). Teflon-lined aluminum or stainless-steel tubing was used to handle the gases in all parts of the system that came in contact with hydrazine, outside of the pyrex reaction apparatus.

A schematic diagram of the apparatus is shown in Figure 1. The hydrazine/N_2 mixture was mixed with O_2 and more N_2 in a tubular region approximately 1.5 m upstream from the reaction site. Calibrated mass flow meters (MKS-SK series) were used to measure the flow rate of each gas into the reaction cell. The total pressure in the cell was measured with either a 10- or 100-Torr capacitance manometer (Edwards Datametrics Barocel). Data were obtained at room temperature, under two flow conditions, for each type of hydrazine. Low-pressure measurements (1 to 3 Torr total pressure) corresponding to relatively fast flows of approximately 300 cm s^{-1} were made to observe the reaction under very dilute reactant conditions. Measurements near 50 Torr were made with a quasi-static flow of approximately 5 cm s^{-1} in a manner analogous to a flash-photolysis resonance fluorescence system. In both cases, the flow was fast enough to completely replenish the reactant mixture between laser pulses. Typical hydrazine concentrations were in the 10^{12} to 10^{13} molecule cm^{-3} range for the low-pressure experiments and in the 10^{13} to 10^{14} molecule cm^{-3} range for the high-pressure experiments. The O_2 concentrations were in the 10^{16} molecule cm^{-3} range.

7

As illustrated in Figure 1, a multiple-port reaction cell was attached to the mixing tube. Oxygen atoms were produced *in situ* from O_2, by 157 nm photolysis using a pulsed F_2 laser (Lambda Physik, Model EMG101) with a typical repetition rate of 2.5 to 5 Hz. The laser was directed perpendicular to the gas flow through the center of the reaction cell. The final spot size of the laser pulse after passing through a series of reducing slits was approximately 2 mm^2, corresponding to a reduced energy per pulse of a fraction of a millijoule. Typical O atom concentrations produced in this manner were 10^{10} to 10^{11} molecule cm^{-3}. A low-pressure atomic oxygen resonance lamp emitting at 131 (^3S - ^3P) nm was directed into the cell, perpendicular to both the bulk flow and the laser beam. The qualities and applicability of this particular type of resonance lamp have been described previously.[11] Ultra-pure helium (Spectra Gases, 99.999%) containing a small oxygen impurity was the gas source for the lamp. Resonance radiation at
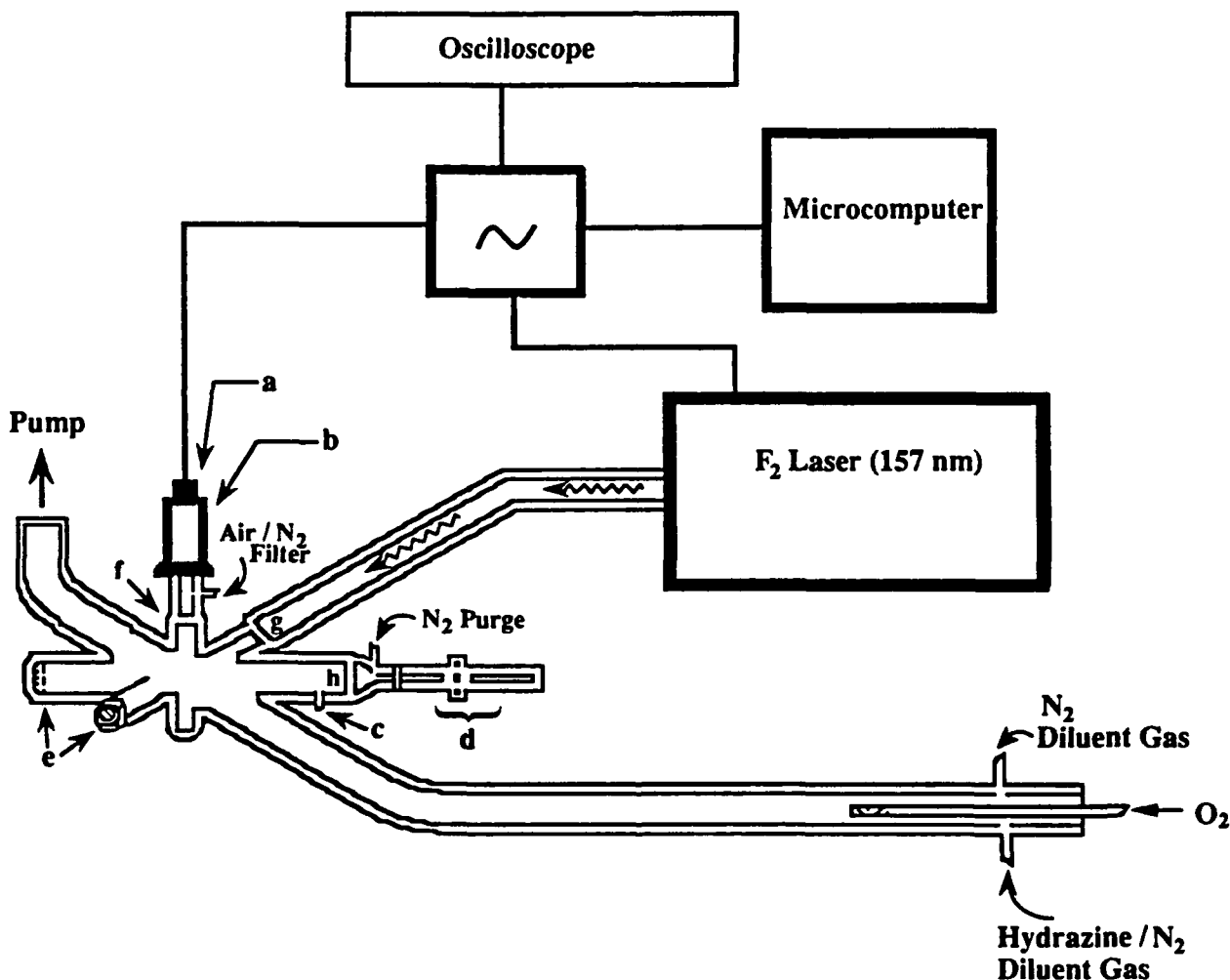

Figure 1. Schematic diagram of the resonance fluorescence apparatus. (a) Preamplifier; (b) Photomultiplier tube; (c) Pressure manometer; (d) O(^3S - ^3P) Resonance lamp; (e) Light baffles; (f) CaF$_2$ window; (g) VUV cultured quartz window; (h) MgF$_2$ window

131 nm from the $O(^3P)$ atoms produced by the laser photolysis was detected perpendicular to both the laser axis and the resonance lamp with a solar blind photomultiplier tube (EMI/GENCOM G-26L314LF). A dry air/N_2 filter in front of the PMT was used to preferentially attenuate the 157-nm radiation from the laser so that it did not interfere with the atomic oxygen signal. The laser pulse was actually much shorter than the time scale of the kinetics measurements so that any residual laser signal could be effectively subtracted from the exponential decay of the fluorescence signal. No delay in the build-up of $O(^3P)$ signal was observed, indicating that the $O(^1D)$ species was rapidly quenched by the N_2 diluent gas if it was produced by the VUV photolysis. N_2 was chosen as the diluent gas because the rate of $O(^1D)$ quenching in N_2[12] is faster than that in other commonly used gases such as He or Ar.[13] Vacuum UV spectra of the hydrazine compounds indicate that approximately 1% of the 157-nm laser intensity would be absorbed by the hydrazine in the cell, and a fraction of that would lead to photodissociation.[14, 15] Since a large excess of hydrazine was present in the system, the amount of hydrazine lost to photolysis was relatively insignificant. In preliminary experiments, the laser intensity was varied over several experiments. Consistent rate constant data for the primary reaction of O atoms with hydrazine was obtained in all cases. Therefore, secondary effects of hydrazine photolysis products reacting with O atoms were also insignificant.

The current from the photomultiplier tube was fed into a custom-built, low-capacitance preamplifier designed to avoid temporal distortion of the fluorescence signal. The signal from the preamp was digitized (LeCroy TR8818 digitizer) and stored with a microcomputer. An external pulse generator provided the time base interval (320 ns to 40 μs) at which points on the intensity curves were recorded. The full-width at half maximum of the laser pulse measured with the PMT was approximately 0.4 μs after amplification while typical fluorescence decays were observed on time scales between 1 and 150 ms. Each fluorescence decay curve was signal averaged over 200 to 500 laser pulses.

RESULTS

The experimental data consisted of decay curves of $O(^3P)$ resonance fluorescence signal intensity as a function of time. Typical raw data curves for the reaction of 1,1- dimethylhydrazine with O atoms are shown in Figure 2.

The change in signal intensity, I, as a function of time, t, is related to the depletion of O atoms by the following rate expression,

$$-\frac{dI}{dt} = -\frac{d\,O(^3P)}{dt} = (k_d + k_2[O_2] [N_2] + k_1[Hyd]) [O(^3P)] = K [O(^3P)] \quad (3)$$
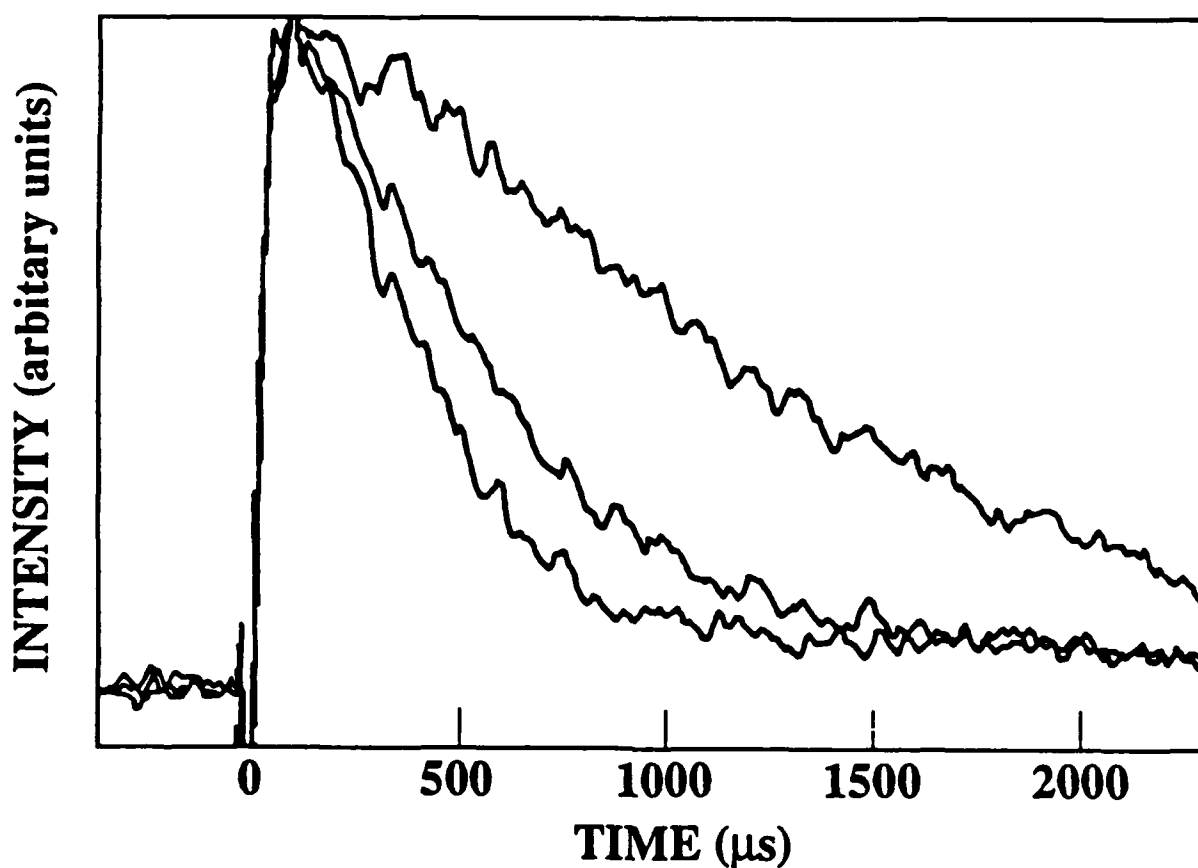

Figure 2. Resonance fluorescence $(O(^3S - ^3P))$ from a monomethyl hydrazine experiment. Total pressure = 53 Torr. Amounts of hydrazine present: (a) 8.65 x 10^{13} molecule cm^{-3}, (b) 1.72 x 10^{14} molecule cm^{-3}, (c) 2.37 x 10^{14} molecule cm^{-3}. Solid lines connect raw data points by interpolation.

where k_d is the first-order rate constant for the loss of O atoms due to diffusion out of the field of view, k_1 is the bimolecular rate constant for the reaction of hydrazine with $O(^3P)$, [Hyd] is the concentration of N_2H_4, $CH_3HN_2H_2$ or $(CH_3)_2N_2H_2$, $[O(^3P)]$ is the concentration of ground-state oxygen atoms and K is the effective first-order rate constant under the pseudo-first-order kinetic conditions. The term, k_2 $[O_2]$ $[N_2]$ has been included in K to account for the loss of O atoms by reaction with O_2 in the three-body reaction,

$$O + O_2 + M \xrightarrow{k_2} O_3 + M,$$ (4)

where $M = N_2$. The termolecular rate constant, k_2, is 6.2×10^{-34} cm^6 $molecule^{-2}$ s^{-1} at 296 K.[16]

The integrated form of Equation (3) can be expressed as,

$$\ln I = \ln \frac{[O(^3P)]_t}{[O(^3P)]_0} = -Kt + c .$$ (5)

Characteristic decay times (τ) were obtained by nonlinear, least-squares fitting of an exponential function to each resonance fluorescence curve. Since $K = 1/\tau$, plotting $1/\tau$ as a function of the hydrazine concentration allowed us to obtain the rate constant for the reaction of hydrazine with $O(^3P)$.

Data plots for experiments performed at several total pressures are shown in Figures 3 and 4. For any given total pressure, with constant N_2 and O_2 flow rates, plots of $1/\tau$ vs. [Hyd] are essentially linear. The intercept is equal to the rate constant for the diffusion of O atoms out of the field of view plus the loss by collision with O_2. Generally, for the experiments performed at 1 to 3 Torr, the rate of loss of $O(^3P)$ atoms by Reaction (4) is small (~ 0.1 s^{-1}) compared to the diffusive loss from the field of view (30 - 40 s^{-1}). However, for the high-pressure experiments, performed near 50 Torr, a contribution of ~ 20 s^{-1} comes from the reaction with O_2 since a considerable amount of N_2 was added to the system. When hydrazine is added to the high-pressure system, the rate of consumption of $O(^3P)$ atoms by hydrazine is 100 times faster than the consumption by O_2, so this mechanism dominates the depletion. The result is that a small deviation from linearity (the pure diffusion plus hydrazine reaction case is linear) occurs at the intercept. This is not evident on the scale depicted in Figure 4.

One difference between the low-pressure fluorescence decay data and the high-pressure data was that the former contained a contribution to the signal from rapid bulk flow past the PMT window. This bulk velocity component was temporally separable from the exponential diffusion decay since it was considerably faster and remained constant for a given total flow and pressure. Only the diffusive portion of the data was used in our analysis. The other effect of this second type of decay was a reduction in the initial intensity of the curves used for our measurements. Both the amplitude and the temporal effects were well characterized for a given set of flow condi-

12

tions. The measured low-pressure rate constants were not statistically different from the high-pressure results.

Since the total pressure changed as hydrazine was added to the flow (this affects the decay time), the times were linearly corrected when the pressure changed by more than approximately 1%. Without this correction, the decay curve from which the $1/\tau$ intercept is obtained may represent slightly different pressure conditions than the data obtained when hydrazine was added. The correction to constant pressure for all decay curves was only necessary for the high-pressure data, and generally the correction was less than 5%.
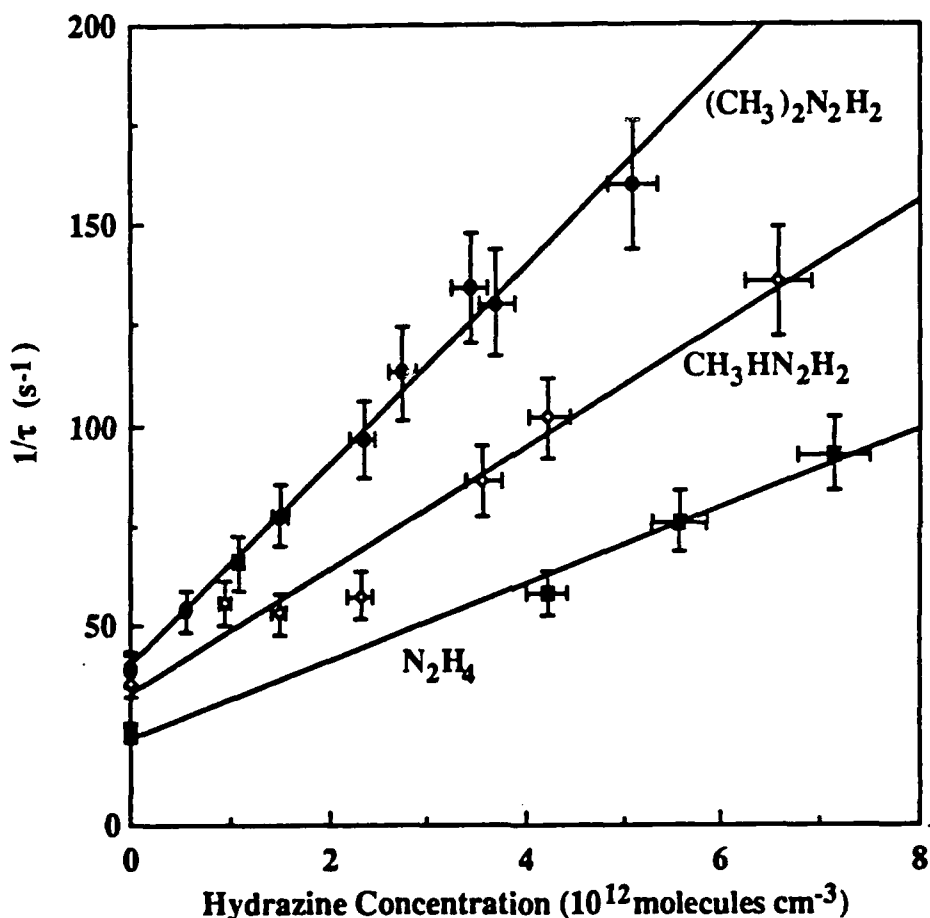

Figure 3. Data from typical low-pressure experiments. The effective first order rate constant ($K = 1/\tau$) is plotted as a function of the hydrazine concentration. Actual pressures were 2 Torr (N_2H_4) and 1 Torr ($CH_3HN_2H_2$ and $(CH_3)_2N_2H_2$). Slopes are reported as k_1 in Table 1.

The room temperature rate constants from several experiments performed at pressures of 1 to 3 Torr and at approximately 50 Torr are listed in Table 1. The results have been averaged for each type of hydrazine to give the final rate constants of 0.99 ($\pm$ 0.12) x 10^{-11} cm^3 molecule^{-1} s^{-1} for N_2H_4, 1.6 ($\pm$ 0.34) x 10^{-11} cm^3 molecule^{-1} s^{-1} for $CH_3HN_2H_2$, and 2.1 $\pm$ (0.34) x 10^{-11} cm^3 molecule^{-1} s^{-1} for $(CH_3)_2N_2H_2$ where the errors quoted are at the 95% confidence level.

A maximum error of $\pm$ 10% in the value of τ is estimated. In order to record the high-pressure data, it was necessary to switch the time base range of the digitizer several times within a single experiment in order to capture successively shorter decay curves as hydrazine reacted with the O atoms. The time interval was independently measured with an oscilloscope; however, small uncertainties in a single time interval are multiplied by the number of channels used to record the signal (nominally 3584). Furthermore, there is an inherent uncertainty associated with the exponential fitting, depending on the signal-to-noise ratio of individual data sets. The errors associated with the hydrazine concentrations are estimated to be $\pm$ 5% from the pressure and mass flow measurements.
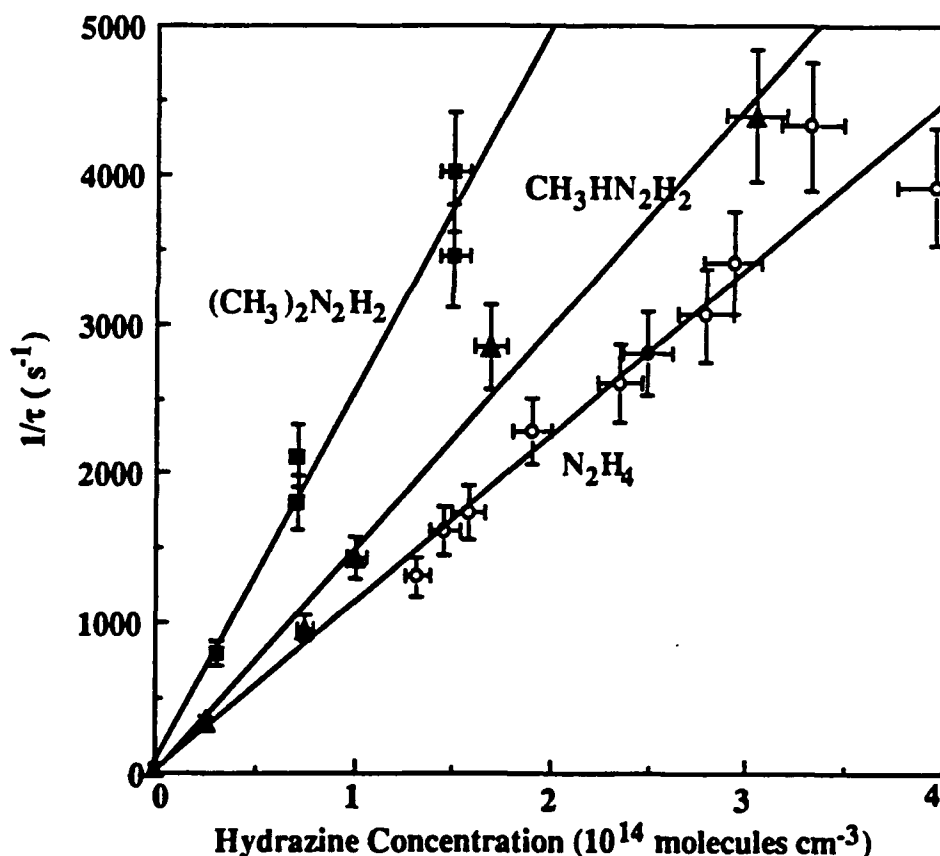

Figure 4. Data from typical high-pressure experiments. The effective first-order rate constant (K = $1/\tau$) is plotted as a function of the hydrazine concentration. Actual pressures were 55 Torr (N_2H_4) and 48 Torr ($CH_3HN_2H_2$ and $(CH_3)_2N_2H_2$). Slopes are reported as k_1 in Table 1.

14

Table 1. Room Temperature Rate Constants for the Reactions of Hydrazine Fuels with O(^{3}P).

N_2H_4		$CH_3HN_2H_2$		$(CH_3)_2N_2H_2$	
PRESSURE (Torr)	RATE CONSTANT (10^{-11} cm^3 molecule^{-1} s^{-1})	PRESSURE (Torr)	RATE CONSTANT (10^{-11} cm^3 molecule^{-1} s^{-1})	PRESSURE (Torr)	RATE CONSTANT (10^{-11} cm^3 molecule^{-1} s^{-1})
1	0.944	1	2.12	1	2.48
1	1.02	2	1.69	1	2.52
2	1.27	3	1.76	2	1.86
3	1.03	1	2.18	3	2.36
1	0.953	1	1.21	53	2.55
2	1.04	2	1.20	51	1.74
2.6	0.911	3	1.48	48	2.46
1	0.817	1	1.53		
2	0.964	48	1.49		
2.3	0.860	53	1.40		
55	1.11				
11 Expts.	Average = 0.99 ± 0.12	10 Expts.	Average = 1.6 ± 0.34	7 Expts.	Average = 2.3 ± 0.34

DISCUSSION

Comparing our rate constant for the reaction of N_2H_4 with O atoms to that previously reported by Gehring et al.,[4,5] it is apparent that their value of 1.4×10^{-11} cm^3 molecule^{-1} s^{-1} is somewhat higher than our result of $0.99 (\pm 0.12) \times 10^{-11}$ cm^3 molecule^{-1} s^{-1}. Limitations associated with the general flow tube method used by Gehring et al. could account for the majority of the difference between the reported rate constants.[17] Several minor complications associated with the previously reported rate constant for N_2H_4 were considered in designing our experimental system. The Gehring et al. experiments were performed with an excess of O atoms relative to hydrazine. Using their mass spectrometric technique, they monitored the loss of N_2H_4 parent molecules during the experiment and only the relative build-up of product species. Even though the experimental mixtures of N_2H_4 were dilute (0.1 to 1% in carrier gas) the loss of hydrazine in surface reactions was not investigated. Heterogeneous hydrazine losses would lead to an apparent rate constant with O atoms that was too high. Other possible channels for the consumption of hydrazine are the reaction with $O_2(^1\Delta)$ and, to a lesser extent, the reaction with $O(^1D)$. Both of these excited species are produced along with $O(^3P)$ when the source is O_2 passed through a microwave discharge.[18,19] While the percentage of excited species produced is considerably less than that of the ground-state product $O(^3P)$, the rate constants for hydrazine reactions with the energetic species $O(^1D)$ is expected to be significantly larger,[20] approaching gas kinetic. Each of these mechanisms for hydrazine loss would result in an observed bimolecular rate constant that was erroneously large in an experiment where only hydrazine was monitored. The rate constant reported by Shane and Brennan[6] was reported as an estimate since the primary goal of their experiments was identification of product species. One reason that it may only have been an estimate is that the method of monitoring product species did not preclude secondary reactions of those species, particularly those of NH_2 and OH, with hydrazine.

The rate constants reported here for the reactions of hydrazine compounds with $O(^3P)$ atoms follow the trend k_1 $(CH_3)_2N_2H_2$ > k_1 $CH_3HN_2H_2$ > k_1 N_2H_4 at room temperature. The ratios of the rate constants are close to that of the number of hydrogens per molecule. Since the mechanisms for the primary reactions of $(CH_3)_2N_2H_2$ and $CH_3HN_2H_2$ are still under investigation,[8] it would be premature to associate these rate coefficients with a simple hydrogen abstraction mechanism for all cases. The fact that our rate constants increase with the number of hydrogen atoms in the hydrazine molecule may simply reflect the stabilizing effect of adjacent methyl groups on the radical intermediates formed when a single hydrogen atom is removed. Further kinetic and mechanistic experiments with 1,2-dimethylhydrazine, $CH_3HN_2HCH_3$, will help to elucidate the primary reaction step for the methylated derivatives with $O(^3P)$.

Since the temperature of the upper atmosphere, above 150 km, is nominally between 600 and 1000 K,[21] it would be instructive to perform temperature studies of the rate coefficients used to model high-altitude hydrazine reactions. The room-temperature rate constants for the hydrazines with $O(^3P)$ are relatively fast; therefore, it is expected that as the temperature of the system is increased, the rates will approach a gas kinetic limit. Only a nominal increase in temperature in these systems is experimentally accessible before the parent hydrazine compounds decompose.

17

CONCLUSION

This study provides room-temperature measurements of rate constants for the reactions of hydrazine, methylhydrazine, and 1,1-dimethylhydrazine with $O(^3P)$ atoms. The experimentally determined values at 296 K are 0.99 ($\pm$ 0.12) x 10^{-11} cm^3 molecule^{-1} s^{-1}, 1.6 ($\pm$ 0.34) x 10^{-11} cm^3 molecule^{-1} s^{-1}, and 2.3 ($\pm$ 0.34) x 10^{-11} cm^3 molecule^{-1} s^{-1}, respectively. The $O(^3P)$ resonance fluorescence technique employed here allowed us to study ground-state atomic oxygen unambiguously, in contrast to several previous mechanistic and kinetic studies of these systems, which may have been complicated by excited atomic and molecular oxygen species.

Even though the purpose of this study was the retrieval of kinetic parameters rather than product identification, it is interesting to compare the rate constants with current mechanistic theories concerning the reactions of the various hydrazines with atomic oxygen. There is an apparent correlation between the number of hydrogen atoms on a particular hydrazine molecule and the room-temperature rate constants measured in our study.

The rate constants reported here have fundamental importance in modeling the chemistry of unburned hydrazine fuels that escape into the upper atmosphere from space launch vehicles.

REFERENCES

1) G. E. Moore, K. E. Shuler, S. Silverman, and R. Herman, *J. Phys. Chem.* **1956**, *60*, 813.

2) A. R. Hall and H. G. Wolfhard, *Trans. Faraday Soc.* **1956**, *52*, 1520.

3) K. H. Becker and K. D. Bayes, *J. Phys. Chem.* **1967**, *71*, 371.

4) M. Gehring, K. Hoyermann, H. G. Wagner, and J. Wolfrum, *Ber. Bunsenges. Physik. Chem.* **1969**, *73*, 956.

5) M. Gehring, K. Hoyermann, H. Schacke, and J. Wolfrum,, *Fourteenth Symposium (International) on Combustion*; The Combustion Institute: Pittsburgh, 1972; pp. 99-105.

6) E. C. Shane and W. Brennen, *J. Chem. Phys.* **1971**, *55*, 1479.

7) S. N. Foner and R. L. Hudson, *J. Chem. Phys.* **1970**, *53*, 4377.

8) W. L. Dimpfl, L. S. Bernstein, S. M. Adler-Golden, J. W. Cox, K. W. Cunningham, and A.T. Pritt, *Proceedings of the 1991 JANNAF (Joint Army-Navy-NASA-Air Force) Exhaust Plumes Technology Subcommittee Meeting*, Laurel, MD, May 1991.

9) E. Cadwallader and L.B. Piper, *Hydrazine Compatibility Survey*; Chemical Propulsion Information Agency: Silver Springs, MD, 1973.

10) E. W. Schmidt, *Hydrazine and Its Dervatives: Preparation, Properties, Applications*; John Wiley and Sons: New York, 1984; pp. 454-483.

11) D. Davis and W. Braun, *Appl. Opt.* **1968**, *7*, 2071.

12) G. E. Streit, C.J. Howard, A.L. Schmeltekopf, J. A. Davidson, and H. I. Schiff, *J. Chem. Phys.* **1976**, *65*, 4761.

13) J. A. Davidson, H. I. Schiff, T. J. Brown, G. E. Streit, and C. J. Howard, *J. Chem. Phys.* **1978**, *69*, 1213.

14) M. Schurgers and K. H. Welge, *Z. Naturforsch* **1968**, *23a*, 1508.

15) H. Biehl and F. Stuhl, *J. Photochem. Photobiol. A: Chem.* **1991**, *59*, 135.

16) Recommended by NASA panel evaluation, W. B. DeMore, M. J. Molina, S.P. Sander, D.M. Golden, R.F. Hampson, M.J. Kurylo, C.J. Howard, and A. R. Ravishankara, *Chemical Kinetics and Photochemical Data for Use in Stratospheric Modeling*; Evaluation Number 8; JPL Publication 87-41, NASA Jet Propulsion Laboratory: Pasadena, CA, 1987, pp. 81 and references contained therein.

17) C. J. Howard, *J. Phys. Chem.* **1979**, *83*, 3.

18) J. P. Doering, E.E. Gulcicek, and S.O. Vaughan, *Chem. Phys. Lett.* **1985**, *114*, 334.

19) R. G. Derwent and B. A. Thrush, *Trans. Faraday Soc.* **1971**, *67*, 2036.

20) Recommended by NASA panel evaluation, W. B. DeMore, M. J. Molina, S.P. Sander, D.M. Golden, R.F. Hampson, M.J. Kurylo, C.J. Howard and A. R. Ravishankara, *Chemical Kinetics and Photochemical Data for Use in Stratospheric Modeling*; Evaluation Number 8; JPL Publication 87-41, NASA Jet Propulsion Laboratory: Pasadena, CA, 1987, pp. 29-30 and references contained therein.

21) *"U.S. Standard Atmosphere, 1976"*, National Oceanic and Atmospheric Administration: Washington, DC, 1976, pp. 69-73.

TECHNOLOGY OPERATIONS

The Aerospace Corporation functions as an "architect-engineer" for national security programs, specializing in advanced military space systems. The Corporation's Technology Operations supports the effective and timely development and operation of national security systems through scientific research and the application of advanced technology. Vital to the success of the Corporation is the technical staff's wide-ranging expertise and its ability to stay abreast of new technological developments and program support issues associated with rapidly evolving space systems. Contributing capabilities are provided by these individual Technology Centers:

Electronics Technology Center: Microelectronics, solid-state device physics, VLSI reliability, compound semiconductors, radiation hardening, data storage technologies, infrared detector devices and testing; electro-optics, quantum electronics, solid-state lasers, optical propagation and communications; cw and pulsed chemical laser development, optical resonators, beam control, atmospheric propagation, and laser effects and countermeasures; atomic frequency standards, applied laser spectroscopy, laser chemistry, laser optoelectronics, phase conjugation and coherent imaging, solar cell physics, battery electrochemistry, battery testing and evaluation.

Mechanics and Materials Technology Center: Evaluation and characterization of new materials: metals, alloys, ceramics, polymers and their composites, and new forms of carbon; development and analysis of thin films and deposition techniques; nondestructive evaluation, component failure analysis and reliability; fracture mechanics and stress corrosion; development and evaluation of hardened components; analysis and evaluation of materials at cryogenic and elevated temperatures; launch vehicle and reentry fluid mechanics, heat transfer and flight dynamics; chemical and electric propulsion; spacecraft structural mechanics, spacecraft survivability and vulnerability assessment; contamination, thermal and structural control; high temperature thermomechanics, gas kinetics and radiation; lubrication and surface phenomena.

Space and Environment Technology Center: Magnetospheric, auroral and cosmic ray physics, wave-particle interactions, magnetospheric plasma waves; atmospheric and ionospheric physics, density and composition of the upper atmosphere, remote sensing using atmospheric radiation; solar physics, infrared astronomy, infrared signature analysis; effects of solar activity, magnetic storms and nuclear explosions on the earth's atmosphere, ionosphere and magnetosphere; effects of electromagnetic and particulate radiations on space systems; space instrumentation; propellant chemistry, chemical dynamics, environmental chemistry, trace detection; atmospheric chemical reactions, atmospheric optics, light scattering, state-specific chemical reactions and radiative signatures of missile plumes, and sensor out-of-field-of-view rejection.